MS. THESIS

Ergodic Capacity Analysis in an Energy Harvesting Cooperative NOMA Network

에너지 하베스팅을 사용하는 비직교 다중접속 기반 협력 네트워크의 에르고딕 용량 분석

BY

Changhyun Kim

February 2019

DEPARTMENT OF ELECTRICAL AND
COMPUTER ENGINEERING
COLLEGE OF ENGINEERING
SEOUL NATIONAL UNIVERSITY

Abstract

Ergodic Capacity Analysis in an Energy Harvesting Cooperative NOMA Network

Changhyun Kim

Department of Electrical and Computer Engineering

The Graduate School

Seoul National University

Non-orthogonal multiple access (NOMA) is a promising technology for the fifth generation (5G) wireless communication systems. NOMA improves the system capacity and user fairness compared to the conventional orthogonal multiple access (OMA). Cooperative communication is widely used to extend the communication range and reception reliability. Energy harvesting (EH) is an efficient way to the improve energy efficiency of the network.

In this thesis, we investigate a cooperative NOMA network with a decode-and-forward (DF) relay which harvests energy from the received signal using power splitting. A relay deployed in the network helps the transmission from the source to the users. Channel order indicator is adopted to ensure that more power is allocated to the instantaneous weak user. We derive the analytical expressions for the end-to-end ergodic capacities between the source and the users. Simulation results show that the ergodic capacities of the users increase as the source transmit power increases. It is also shown that the end-to-end ergodic capacity from the source to the user closer to the relay decreases as the power allocation coefficient for the weak user increases while that from the source to the user farther to the relay increases.

Keywords: Ergodic capacity, cooperative NOMA, energy harvesting, decode-and-forward, power splitting.

Student Number: 2017-23534.

Contents

List of Figures

Chapter 1

Introduction

Non-orthogonal multiple access (NOMA) has been considered as a promising candidate technology for the fifth generation (5G) wireless communication networks due to its superior spectral efficiency over conventional orthogonal multiple access (OMA) [1]. In NOMA, multiple users are served in the same frequency, time, and coding domain, by using power domain user multiplexing at the transmitter and successive interference cancellation (SIC) at the receiver [2].

Cooperative relay transmission has been applied to wireless communication networks to extend the communication range and reception reliability of the systems [3]-[5]. With an aid of the relay, the deterioration of the source-to-user links, which is the result of the deep fading or severe path loss, can be overcome [6]. In cooperative NOMA networks, relays deployed in the network help the transmission between the source and the users using NOMA [7]. When cooperative transmission is applied to NOMA systems, the outage performance and sum capacity are improved in [8] and [9], respectively.

Energy harvesting (EH) is another key technology for 5G wireless communication systems as energy-efficient communications gain more prominence due to energy shortage, recently [10]. EH is an efficient way to prolong the lifetime of the energy-constrained wireless networks because EH nodes harvest energy from their received signal and do not need to change a battery [11]. As Internet of Things (IoT) emerges as one of the hottest technology for future wireless networks, stable energy supply to such nodes becomes important [12]. Recently, EH has also applied to cooperative NOMA networks. [13]-[18]

Most of previous works on the EH cooperative NOMA focus on the outage probability. In [13], the outage probability of the EH cooperative NOMA system was derived. In [14], the impact of the power allocation on EH cooperative NOMA networks was investigated. In [15], the outage probability of the EH cooperative NOMA network with transmit antenna selection was derived. In [16], the outage probabilities for the EH cooperative NOMA networks with transmit antenna selection and maximum ratio combining (MRC) are derived over Nakagami-m fading channels.

Ergodic capacity is one of the most important performance measures in wireless communications, as it shows the long-term average transmission rate of the network in a fading environment. There were few works on the ergodic capacity of EH cooperative NOMA networks [17], [18]. However, they only investigated amplify-and-forward (AF) relay networks where only outage capacities are obtained. To the best of our knowledge, there is no work that investigated the ergodic capacity of the decode-and-forward (DF) relay network.

In this thesis, we investigate a cooperative NOMA network with a decode-and-forward (DF) relay which harvests energy from the received signal using power splitting (PS). A relay deployed in the network helps the transmissions from the source to the users. We derive the analytical expressions for the end-to-end ergodic capacity between the source and the users. We adopt a channel order indicator to ensure that more power is allocated to the instantaneous weak user according to the NOMA principle. The instantaneous signal to interference-plus-noise ratio (SINR) expression is obtained for each link and the CDFs of the SINRs are derived. Then the closed-form expression of the ergodic capacities are obtained.

The rest of this paper is organized as follows. In chapter 2, the system model is described. In chapter 3, the end-to-end ergodic capacity is analyzed. In chapter 4, simulation results are shown. Finally, conclusions are drawn in chapter 5.

Chapter 2

System Model

Consider a downlink cooperative non-orthogonal multiple access (NOMA) network with one source S, one decode-and-forward (DF) relay R, and two users D_1 and D_2. Suppose that all nodes are equipped with a single antenna and operate in a half-duplex mode. Assume that there is no direct link between the source and the users.

Assume that the channel coefficient between nodes i and j, $h_{i,j}$, $i, j \in \{S, R, D_1, D_2\}$, is an independent circularly symmetric complex

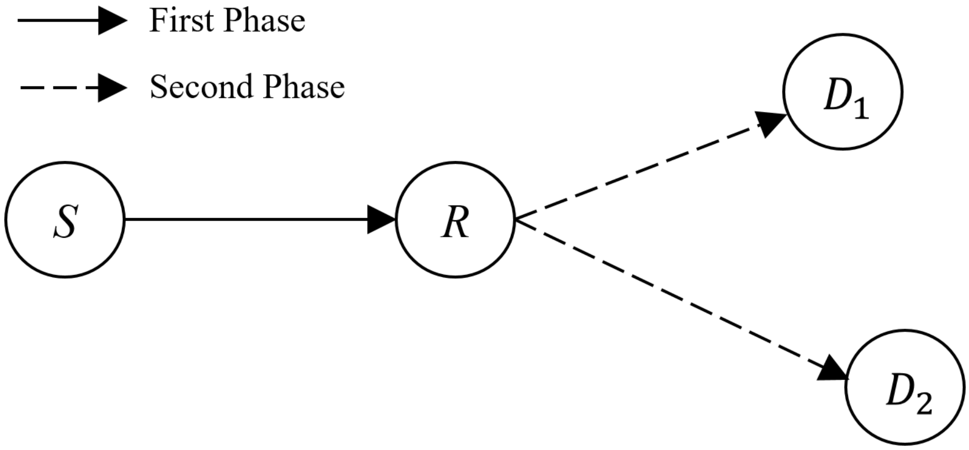

Figure 2.1. Downlink EH cooperative NOMA system.

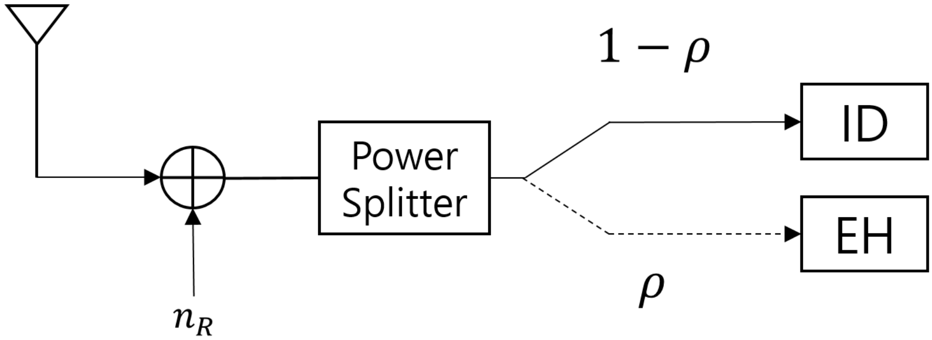

Figure 2.2. A diagram of the power splitting relay.

Gaussian random variable with zero mean and variance $d_{i,j}^{-v}$, where v is the path loss exponent and $d_{i,j}$ is the distance between nodes i and j. Define the channel gain between the nodes i and j as $|h_{i,j}|^2$. The probability density function of $|h_{i,j}|^2$ is given by

$$f_{|h_{i,j}|^2}(x) = d_{i,j}^{v} e^{-d_{i,j}^{v} x}. \tag{2.1}$$

Assume that each channel has an additive white Gaussian noise (AWGN) with zero mean and variance σ^2.

Suppose that the source transmits a signal to the two users in two time slots, where each of its duration is normalized to one. In the first time slot, the source superimposes signals for D_1 and D_2. Let denote the user with the larger channel gain as a strong user and the user with the smaller channel gain as a weak user. If D_1 is a weak user, i.e., $|h_{R,D_1}|^2 \le |h_{R,D_2}|^2$, $\delta = 1$. If $|h_{R,D_1}|^2 > |h_{R,D_2}|^2$, $\delta = 0$.

The transmitted signal from the source is given by

$$x_S = \delta\sqrt{P_S}\left(\sqrt{\alpha_w}x_1 + \sqrt{\alpha_s}x_2\right) + (1-\delta)\sqrt{P_S}\left(\sqrt{\alpha_s}x_1 + \sqrt{\alpha_w}x_2\right), \tag{2.2}$$

where P_S is the transmit power of the source, α_w and α_s are the power allocation coefficients for the weak and strong users, with $\alpha_w + \alpha_s = 1$, $\alpha_w > \alpha_s$ according to the NOMA principle, and x_1 and x_2 are the signals for D_1 and D_2, respectively. The received signal at the relay is given by

$$y_R = h_{S,R} x_S + n_R, \tag{2.3}$$

where n_R is an AWGN at the relay. Suppose that the relay does not have its own power supply and harvests energy from the received signal based on power splitting. Let $\rho,\ 0<\rho<1,$ denote the power splitting ratio. The received signal power is split into two portions: portion ρ for EH and portion $1-\rho$ for information decoding. The harvested energy at the relay in the first time slot is given by

$$E_R = \eta\rho P_S |h_{S,R}|^2, \tag{2.4}$$

where $\eta,\ 0 \le \eta \le 1,$ is the energy conversion efficiency. The relay decodes the signal of the weak user directly by treating the signal of the strong user as a noise and decodes the signal of the strong user without interference after successive interference cancellation (SIC). The received signal to interference-plus-noise ratio (SINR) at the relay to detect x_1 is given by

$$\gamma_R^{x_1} = \delta\left(\frac{(1-\rho)\alpha_w P_S |h_{S,R}|^2}{(1-\rho)\alpha_s P_S |h_{S,R}|^2 + \sigma^2}\right) + (1-\delta)\left(\frac{(1-\rho)\alpha_s P_S |h_{S,R}|^2}{\sigma^2}\right). \tag{2.5}$$

The received SINR at the relay to detect x_2 is given by

$$\gamma_R^{x_2} = (1-\delta)\left(\frac{(1-\rho)\alpha_w P_S |h_{S,R}|^2}{(1-\rho)\alpha_s P_S |h_{S,R}|^2 + \sigma^2}\right) + \delta\left(\frac{(1-\rho)\alpha_s P_S |h_{S,R}|^2}{\sigma^2}\right). \tag{2.6}$$

In the second time slot, the relay re-encodes the decoded signals to transmit them to D_1 and D_2, which is given by

$$x_R = \delta\sqrt{P_R}\left(\sqrt{\beta_w}x_1 + \sqrt{\beta_s}x_2\right) + (1-\delta)\sqrt{P_R}\left(\sqrt{\beta_s}x_1 + \sqrt{\beta_w}x_2\right), \tag{2.7}$$

where P_R is the transmit power of the relay, and β_w and β_s are the power allocation coefficients for the weak and strong users, respectively, with $\beta_w + \beta_s = 1,\ \beta_w > \beta_s$. Suppose that all energy harvested at the relay is used in the second time slot. The transmit power of the relay is given by

$$\begin{aligned} P_R &= E_R \\ &= \eta\rho P_S\,|h_{S,R}|^2 . \end{aligned} \tag{2.8}$$

The received signal at D_1 is given by

$$y_{D_1} = h_{R,D_1}x_R + n_{D_1}, \tag{2.9}$$

where n_{D_1} is an AWGN at D_1. The received signal at D_2 is given by

$$y_{D_2} = h_{R,D_2}x_R + n_{D_2}, \tag{2.10}$$

where n_{D_2} is an AWGN at D_2. The received SINR at D_1 to detect x_1 is given by

$$\begin{aligned} \gamma_{D_1}^{x_1} = \delta&\left(\frac{\beta_w\eta\rho P_S\,|h_{S,R}|^2|h_{R,D_1}|^2}{\beta_s\eta\rho P_S\,|h_{S,R}|^2|h_{R,D_1}|^2+\sigma^2}\right) \\ &+(1-\delta)\left(\frac{\beta_s\eta\rho P_S\,|h_{S,R}|^2|h_{R,D_1}|^2}{\sigma^2}\right). \end{aligned} \tag{2.11}$$

The received SINR at D_2 to detect x_2 is given by

$$\gamma_{D_2}^{x_2} = (1-\delta)\left(\frac{\beta_w \eta \rho P_S \,|\, h_{S,R} \,|^2 |\, h_{R,D_2} \,|^2}{\beta_s \eta \rho P_S \,|\, h_{S,R} \,|^2 |\, h_{R,D_2} \,|^2 + \sigma^2} \right)$$

$$+\delta \left(\frac{\beta_s \eta \rho P_S \,|\, h_{S,R} \,|^2 |\, h_{R,D_2} \,|^2}{\sigma^2} \right). \tag{2.12}$$

Chapter 3

Ergodic Capacity Analysis

3.1 Ergodic Capacity of the Relay

The instantaneous capacity of the relay to detect x_1 is given by

$$C_R^{x_1} = \log(1+\gamma_R^{x_1}). \tag{3.1}$$

The ergodic capacity of the relay to detect x_1 is given by

$$\begin{aligned}
\bar{C}_R^{x_1} &= \mathbb{E}[C_R^{x_1}] \\
&= \frac{1}{\ln 2}\int_0^\infty \frac{1-F_{\gamma_R^{x_1}}(\gamma)}{1+\gamma} d\gamma \\
&= \Pr\{\delta = 1\} \frac{1}{\ln 2}\int_0^\infty \frac{1-F_{\gamma_R^{x_1}}(\gamma \mid \delta = 1)}{1+\gamma} d\gamma
\end{aligned}$$

$$+\Pr\{\delta=0\}\frac{1}{\ln 2}\int_0^\infty \frac{1-F_{\gamma_R^{x_1}}(\gamma\mid\delta=0)}{1+\gamma}d\gamma, \tag{3.2}$$

where $F_\Gamma(\cdot)$ is the cumulative distribution function (CDF) of Γ. The probability that $\delta=1$ and $\delta=0$ are given by

$$\begin{aligned}\Pr\{\delta=1\} &= \Pr\{|h_{R,D_1}|^2 \le |h_{R,D_2}|^2\} \\ &= \int_0^\infty \int_0^y d_{R,D_1}^\nu e^{-d_{R,D_1}^\nu x} d_{R,D_2}^\nu e^{-d_{R,D_1}^\nu y} dxdy \\ &= \frac{d_{R,D_1}^\nu}{d_{R,D_1}^\nu + d_{R,D_2}^\nu}\end{aligned} \tag{3.3}$$

and

$$\begin{aligned}\Pr\{\delta=0\} &= 1-\Pr\{\delta=1\} \\ &= \frac{d_{R,D_2}^\nu}{d_{R,D_1}^\nu + d_{R,D_2}^\nu},\end{aligned} \tag{3.4}$$

respectively. From (3.2), (3.3), and (3.4), the ergodic capacity of the relay to detect x_1 is given by

$$\begin{aligned}\bar{C}_R^{x_1} &= \frac{d_{R,D_1}^\nu}{d_{R,D_1}^\nu + d_{R,D_2}^\nu}\frac{1}{\ln 2}\underbrace{\int_0^\infty \frac{1-F_{\gamma_R^{x_1}}(\gamma\mid\delta=1)}{1+\gamma}d\gamma}_{X} \\ &+ \frac{d_{R,D_2}^\nu}{d_{R,D_1}^\nu + d_{R,D_2}^\nu}\frac{1}{\ln 2}\underbrace{\int_0^\infty \frac{1-F_{\gamma_R^{x_1}}(\gamma\mid\delta=0)}{1+\gamma}d\gamma}_{Y}.\end{aligned} \tag{3.5}$$

From (2.1) and (2.5), the conditional CDF of $\gamma_R^{x_1}$ given $\delta=1$ is given by

$$F_{\gamma_R^{x_1}}(\gamma \mid \delta=1) = \Pr\left\{ \frac{(1-\rho)\alpha_w P_S \mid h_{S,R} \mid^2}{(1-\rho)\alpha_s P_S \mid h_{S,R} \mid^2 + \sigma^2} \le \gamma \right\}$$

$$= \int_0^{\frac{\sigma^2\gamma}{(1-\rho)P_S(\alpha_w - \alpha_s\gamma)}} d_{S,R}^{\nu} e^{-d_{S,R}^{\nu} x} dx$$

$$= 1 - \mathbf{1}_{\left[0,\frac{\alpha_w}{\alpha_s}\right]}(\gamma) e^{-\frac{d_{S,R}^{\nu}\sigma^2\gamma}{(1-\rho)P_S(\alpha_w - \alpha_s\gamma)}}, \tag{3.6}$$

where $\mathbf{1}_A(x)$ is the indicator function which is given by

$$\mathbf{1}_A(x) = \begin{cases} 1, & \text{if } x \in A, \\ 0, & \text{if } x \notin A. \end{cases} \tag{3.7}$$

From (3.6) and [11, eq. 6.114.3], the integral in the first term on the right hand side of (3.5) is given by

$$X = \int_0^{\infty} \frac{1 - F_{\gamma_R^{x_1}}(\gamma \mid \delta=1)}{1+\gamma} d\gamma$$

$$= \int_0^{\frac{\alpha_w}{\alpha_s}} \frac{e^{-\frac{d_{S,R}^{\nu}\sigma^2\gamma}{(1-\rho)P_S(\alpha_w - \alpha_s\gamma)}}}{1+\gamma} d\gamma$$

$$= e^{\frac{d_{S,R}^{\nu}\sigma^2}{(1-\rho)P_S\alpha_s}} \mathrm{Ei}\left(\frac{d_{S,R}^{\nu}\sigma^2}{(1-\rho)P_S\alpha_s} \right) - e^{\frac{d_{S,R}^{\nu}\sigma^2}{(1-\rho)P_S}} \mathrm{Ei}\left(\frac{d_{S,R}^{\nu}\sigma^2}{(1-\rho)P_S} \right), \tag{3.8}$$

where $\mathrm{Ei}(\cdot)$ is the exponential integral function which is given by $\mathrm{Ei}(x) = -\int_{-x}^{\infty} \frac{e^{-t}}{t} dt$. The conditional CDF of $\gamma_R^{x_1}$ given $\delta = 0$ is given by

$$F_{\gamma_R^{x_1}}(\gamma \mid \delta=0) = \Pr\left\{ \frac{(1-\rho)\alpha_s P_S \mid h_{S,R} \mid^2}{\sigma^2} \le \gamma \right\}$$

$$= \Pr\left\{ |h_{S,R}|^2 \le \frac{\sigma^2\gamma}{(1-\rho)P_S\alpha_s} \right\}$$

$$= \int_0^{\frac{\sigma^2\gamma}{(1-\rho)P_S\alpha_s}} d_{S,R}^{\nu} e^{-d_{S,R}^{\nu}x} dx$$

$$= 1 - e^{-\frac{d_{S,R}^{\nu}\sigma^2\gamma}{(1-\rho)P_S\alpha_s}}. \tag{3.9}$$

From [11, eq.6.114.3], the integral in the second term on the right hand side of (3.5) is given by

$$Y = \int_0^{\infty} \frac{1 - F_{\gamma_R^{x_1}}(\gamma \mid \delta = 0)}{1+\gamma} d\gamma$$

$$= \int_0^{\infty} \frac{e^{-\frac{d_{S,R}^{\nu}\sigma^2\gamma}{(1-\rho)P_S\alpha_s}}}{1+\gamma} d\gamma$$

$$= -e^{\frac{d_{S,R}^{\nu}\sigma^2\gamma}{(1-\rho)P_S\alpha_s}} \mathrm{Ei}\left(-\frac{d_{S,R}^{\nu}\sigma^2\gamma}{(1-\rho)P_S\alpha_s} \right). \tag{3.10}$$

From (3.5), (3.8), and (3.10), the ergodic capacity of the relay to detect x_1 is given by

$$C_R^{x_1} = \frac{d_{R,D_1}^{\nu}}{d_{R,D_1}^{\nu} + d_{R,D_2}^{\nu}} \frac{1}{\ln 2}$$
$$\times \left\{ e^{\frac{d_{S,R}^{\nu}\sigma^2}{(1-\rho)P_S\alpha_s}} \mathrm{Ei}\left(\frac{d_{S,R}^{\nu}\sigma^2}{(1-\rho)P_S\alpha_s} \right) - e^{\frac{d_{S,R}^{\nu}\sigma^2}{(1-\rho)P_S}} \mathrm{Ei}\left(\frac{d_{S,R}^{\nu}\sigma^2}{(1-\rho)P_S} \right) \right\}$$
$$- \frac{d_{R,D_2}^{\nu}}{d_{R,D_1}^{\nu} + d_{R,D_2}^{\nu}} \frac{1}{\ln 2} e^{\frac{d_{S,R}^{\nu}\sigma^2\gamma}{(1-\rho)P_S\alpha_s}} \mathrm{Ei}\left(-\frac{d_{S,R}^{\nu}\sigma^2\gamma}{(1-\rho)P_S\alpha_s} \right). \tag{3.11}$$

Similarly, the ergodic capacity of the relay to detect x_2 is given by

$$
\begin{aligned}
C_R^{x_1} = {} & \frac{d_{R,D_2}^{\nu}}{d_{R,D_1}^{\nu} + d_{R,D_2}^{\nu}} \frac{1}{\ln 2} \\
& \times \left\{ e^{\frac{d_{S,R}^{\nu}\sigma^2}{(1-\rho)P_S\alpha_s}} \mathrm{Ei}\left(\frac{d_{S,R}^{\nu}\sigma^2}{(1-\rho)P_S\alpha_s} \right) - e^{\frac{d_{S,R}^{\nu}\sigma^2}{(1-\rho)P_S}} \mathrm{Ei}\left(\frac{d_{S,R}^{\nu}\sigma^2}{(1-\rho)P_S} \right) \right\} \\
& - \frac{d_{R,D_1}^{\nu}}{d_{R,D_1}^{\nu} + d_{R,D_2}^{\nu}} \frac{1}{\ln 2} e^{\frac{d_{S,R}^{\nu}\sigma^2\gamma}{(1-\rho)P_S\alpha_s}} \mathrm{Ei}\left(-\frac{d_{S,R}^{\nu}\sigma^2\gamma}{(1-\rho)P_S\alpha_s} \right).
\end{aligned} \tag{3.12}
$$

Note that $\bar{C}_R^{x_2}$ is obtained by exchanging d_{R,D_1} and d_{R,D_2} in $\bar{C}_R^{x_1}$.

3.2 Ergodic Capacities of the Users

The instantaneous capacity of D_1 to detect x_1 is given by

$$C_{D_1}^{x_1} = \log(1+\gamma_{D_1}^{x_1}). \tag{3.13}$$

The ergodic capacity of D_1 to detect x_1 is given by

$$\begin{aligned}\bar{C}_{D_1}^{x_1} &= \mathbb{E}[C_{D_1}^{x_1}] \\ &= \frac{1}{\ln 2}\int_0^\infty \frac{1-F_{\gamma_{D_1}^{x_1}}(\gamma)}{1+\gamma}d\gamma \\ &= \Pr\{\delta=1\}\frac{1}{\ln 2}\int_0^\infty \frac{1-F_{\gamma_{D_1}^{x_1}}(\gamma\,|\,\delta=1)}{1+\gamma}d\gamma \\ &\quad +\Pr\{\delta=0\}\frac{1}{\ln 2}\int_0^\infty \frac{1-F_{\gamma_{D_1}^{x_1}}(\gamma\,|\,\delta=0)}{1+\gamma}d\gamma.\end{aligned} \tag{3.14}$$

From (3.3), (3.4), and (3.14), the ergodic capacity of D_1 to detect x_1 is given by

$$\begin{aligned}\bar{C}_{D_1}^{x_1} &= \frac{d_{R,D_1}^{v}}{d_{R,D_1}^{v}+d_{R,D_2}^{v}}\frac{1}{\ln 2}\underbrace{\int_0^\infty \frac{1-F_{\gamma_{D_1}^{x_1}}(\gamma\,|\,\delta=1)}{1+\gamma}d\gamma}_{Z} \\ &\quad +\frac{d_{R,D_2}^{v}}{d_{R,D_1}^{v}+d_{R,D_2}^{v}}\frac{1}{\ln 2}\underbrace{\int_0^\infty \frac{1-F_{\gamma_{D_1}^{x_1}}(\gamma\,|\,\delta=0)}{1+\gamma}d\gamma}_{W}.\end{aligned} \tag{3.15}$$

The conditional CDF of $\gamma_{D_1}^{x_1}$ given $\delta=1$ is given by

$$
\begin{aligned}
F_{\gamma_{D_1}^{x_1}}(\gamma \mid \delta = 1) &= \Pr\{\gamma_{D_1}^{x_1} \le \gamma \mid \delta = 1\} \\
&= \Pr\left\{ \frac{\beta_w \eta \rho P_S |h_{S,R}|^2 |h_{R,D_1}|^2}{\beta_s \eta \rho P_S |h_{S,R}|^2 |h_{R,D_1}|^2 + \sigma^2} \le \gamma \,\middle|\, \delta = 1 \right\} \\
&= \Pr\left\{ |h_{R,D_1}|^2 \le \frac{\sigma^2 \gamma}{\eta \rho P_S (\beta_w - \beta_s \gamma) |h_{S,R}|^2} \,\middle|\, |h_{R,D_1}| \le |h_{R,D_2}| \right\} \\
&= \int_0^\infty \int_0^{\frac{\sigma^2 \gamma}{\eta \rho P_S (\beta_w - \beta_s \gamma) x}} d_{S,R}^{v} e^{-d_{S,R}^{v} x} d_{R,D_1}^{v} e^{-d_{R,D_1}^{v} x} \\
&\times \Pr\left\{ y \le |h_{R,D_2}| \,\middle\|\, |h_{R,D_1}| \le |h_{R,D_2}| \right\} dy dx \\
&= \int_0^\infty d_{S,R}^{v} e^{-d_{S,R}^{v} x} \left(1 - e^{-\frac{(d_{R,D_1}^{v} + d_{R,D_2}^{v}) \sigma^2 \gamma}{\eta \rho P_S (\beta_w - \beta_s \gamma) x}} \right) dx \\
&\overset{(a)}{=} 1 - \mathbf{1}_{\left[0, \frac{\beta_w}{\beta_s}\right]}(\gamma) \left\{ 2\sqrt{\frac{\kappa \gamma}{\beta_1 - \beta_2 \gamma}} K_1\left(2\sqrt{\frac{\kappa \gamma}{\beta_1 - \beta_2 \gamma}} \right) \right\}, \qquad (3.16)
\end{aligned}
$$

where $K_1(\cdot)$ is the first-order modified Bessel function of the second kind, $\kappa = \frac{d_{S,R}^{v}(d_{R,D_1}^{v} + d_{R,D_2}^{v})\sigma^2}{\eta \rho P_S}$, and (a) follows from [19, eq. 3.324.1]. The integral in the first term on the right hand side of (3.15) is given by

$$
\begin{aligned}
Z &= \int_0^{\frac{\beta_w}{\beta_s}} \frac{2}{1+\gamma} \sqrt{\frac{\kappa \gamma}{\beta_1 - \beta_2 \gamma}} K_1\left(2\sqrt{\frac{\kappa \gamma}{\beta_1 - \beta_2 \gamma}} \right) d\gamma \\
&\overset{(b)}{=} \int_0^\infty \left(\frac{1}{1+t} - \frac{1}{\frac{1}{\beta_2} + t} \right) \sqrt{\kappa t} K_1\left(2\sqrt{\kappa t} \right) dt
\end{aligned}
$$

$$\overset{(c)}{=}\sqrt{\kappa}\int_0^\infty t^{\frac{1}{2}}\left\{(1+t)^{-1}-\left(\frac{1}{\beta_2}+t\right)^{-1}\right\}G_{0,2}^{2,0}\left(\kappa\left|\begin{matrix}\{\ \}\\ \left\{\frac{1}{2},-\frac{1}{2}\right\}\end{matrix}\right.\right)dt, \qquad (3.17)$$

where (b) follows from using integration by substitution with $t=\dfrac{\gamma}{\alpha_1-\alpha_2\gamma}$, (c) follows from [20, eq. 14], and $G_{m,n}^{p,q}(\cdot)$ is the Meijer's G-function [19, eq. 9.301]. By using [19, eq. 7.811.5], we have

$$Z=\sqrt{\kappa}\left\{G_{1,3}^{3,1}\left(\kappa\left|\begin{matrix}\left\{-\frac{1}{2}\right\}\\ \left\{-\frac{1}{2},\frac{1}{2},-\frac{1}{2}\right\}\end{matrix}\right.\right)-\sqrt{\frac{1}{\beta_s}}G_{1,3}^{3,1}\left(\kappa\left|\begin{matrix}\left\{-\frac{1}{2}\right\}\\ \left\{-\frac{1}{2},\frac{1}{2},-\frac{1}{2}\right\}\end{matrix}\right.\right)\right\}. \qquad (3.18)$$

The conditional CDF of $\gamma_{D_1}^{x_1}$ given $\delta=0$ is given by

$$\begin{aligned}
F_{\gamma_{D_1}^{x_1}}(\gamma\,|\,\delta=0)&=\Pr\left\{\gamma_{D_1}^{x_1}\le\gamma\,\middle|\,\delta=0\right\}\\
&=\Pr\left\{|h_{R,D_1}|^2\le\frac{\sigma^2\gamma}{\eta\rho P_S\beta_s|h_{S,R}|^2}\,\middle|\,|h_{R,D_1}|>|h_{R,D_2}|\right\}\\
&=\int_0^\infty\int_0^{\frac{\sigma^2\gamma}{\eta\rho P_s\beta_s x}}d_{S,R}^{\nu}e^{-d_{S,R}^{\nu}x}d_{R,D_1}^{\nu}e^{-d_{R,D_1}^{\nu}y}\\
&\quad\times\Pr\left\{y\le|h_{R,D_2}|\,\middle|\,|h_{R,D_1}|>|h_{R,D_2}|\right\}dydx\\
&=\int_0^\infty d_{S,R}^{\nu}e^{-d_{S,R}^{\nu}x}\left\{\frac{d_{R,D_1}^{\nu}+d_{R,D_2}^{\nu}}{d_{R,D_2}^{\nu}}\left(1-e^{-\frac{d_{R,D_1}^{\nu}\sigma^2\gamma}{\eta\rho P_s\beta_s x}}\right)\right.
\end{aligned}$$

$$-\frac{d_{R,D_1}^{\nu}}{d_{R,D_2}^{\nu}}\left(1-e^{-\frac{(d_{R,D_1}^{\nu}+d_{R,D_2}^{\nu})\sigma^2\gamma}{\eta\rho P_s\beta_s x}}\right)\Bigg\}dx$$

$$=\frac{d_{R,D_1}^{\nu}+d_{R,D_2}^{\nu}}{d_{R,D_2}^{\nu}}\left(1-2\sqrt{\tau\gamma}K_1\left(2\sqrt{\tau\gamma}\right)\right)$$

$$-\frac{d_{R,D_1}^{\nu}}{d_{R,D_2}^{\nu}}\left(1-2\sqrt{\chi\gamma}K_1\left(2\sqrt{\chi\gamma}\right)\right), \tag{3.19}$$

Where $\tau=\frac{d_{S,R}^{\nu}d_{R,D_1}^{\nu}\sigma^2}{\eta\rho P_s\beta_s}$ and $\chi=\frac{d_{S,R}^{\nu}(d_{R,D_1}^{\nu}+d_{R,D_2}^{\nu})\sigma^2}{\eta\rho P_s\beta_s}$. The integral in the second term on the right hand side of (3.15) is given by

$$W=\int_0^{\infty}\frac{2}{1+\gamma}\left\{\frac{d_{R,D_1}^{\nu}+d_{R,D_2}^{\nu}}{d_{R,D_2}^{\nu}}\sqrt{\tau\gamma}K_1\left(2\sqrt{\tau\gamma}\right)-\frac{d_{R,D_1}^{\nu}}{d_{R,D_2}^{\nu}}\sqrt{\chi\gamma}K_1\left(2\sqrt{\chi\gamma}\right)\right\}d\gamma$$

$$=\frac{\sqrt{\tau}}{\ln 2}\frac{d_{R,D_1}^{\nu}+d_{R,D_2}^{\nu}}{d_{R,D_2}^{\nu}}G_{1,3}^{3,1}\left(\tau\left|\begin{matrix}\left\{-\frac{1}{2}\right\}\\ \left\{-\frac{1}{2},\frac{1}{2},-\frac{1}{2}\right\}\end{matrix}\right.\right)$$

$$-\frac{\sqrt{\chi}}{\ln 2}\frac{d_{R,D_1}^{\nu}}{d_{R,D_2}^{\nu}}G_{1,3}^{3,1}\left(\chi\left|\begin{matrix}\left\{-\frac{1}{2}\right\}\\ \left\{-\frac{1}{2},\frac{1}{2},-\frac{1}{2}\right\}\end{matrix}\right.\right). \tag{3.20}$$

From (3.15), (3.18), and (3.20), the ergodic capacity of D_1 to detect x_1 is given by

$$\bar{C}_{D_1}^{x_1} = \frac{d_{R,D_1}^{\nu}}{d_{R,D_1}^{\nu} + d_{R,D_2}^{\nu}} \frac{\sqrt{\kappa}}{\ln 2} \left\{ G_{1,3}^{3,1}\left(\kappa \middle| \begin{matrix} \left\{-\frac{1}{2}\right\} \\ \left\{-\frac{1}{2}, \frac{1}{2}, -\frac{1}{2}\right\} \end{matrix} \right) \right.$$

$$\left. - \sqrt{\frac{1}{\beta_s}} G_{1,3}^{3,1}\left(\kappa \middle| \begin{matrix} \left\{-\frac{1}{2}\right\} \\ \left\{-\frac{1}{2}, \frac{1}{2}, -\frac{1}{2}\right\} \end{matrix} \right) \right\}$$

$$+ \frac{\sqrt{\tau}}{\ln 2} G_{1,3}^{3,1}\left(\tau \middle| \begin{matrix} \left\{-\frac{1}{2}\right\} \\ \left\{-\frac{1}{2}, \frac{1}{2}, -\frac{1}{2}\right\} \end{matrix} \right)$$

$$- \frac{\sqrt{\chi}}{\ln 2} \frac{d_{R,D_1}^{\nu}}{d_{R,D_1}^{\nu} + d_{R,D_2}^{\nu}} G_{1,3}^{3,1}\left(\chi \middle| \begin{matrix} \left\{-\frac{1}{2}\right\} \\ \left\{-\frac{1}{2}, \frac{1}{2}, -\frac{1}{2}\right\} \end{matrix} \right). \tag{3.21}$$

Similarly, the ergodic capacity of D_2 to detect x_2 is given by

$$\bar{C}_{D_1}^{x_1} = \frac{d_{R,D_2}^{\nu}}{d_{R,D_1}^{\nu} + d_{R,D_2}^{\nu}} \frac{\sqrt{\kappa}}{\ln 2} \left\{ G_{1,3}^{3,1}\left(\kappa \middle| \begin{matrix} \left\{-\frac{1}{2}\right\} \\ \left\{-\frac{1}{2}, \frac{1}{2}, -\frac{1}{2}\right\} \end{matrix} \right) \right.$$

$$\left. - \sqrt{\frac{1}{\beta_s}} G_{1,3}^{3,1}\left(\kappa \middle| \begin{matrix} \left\{-\frac{1}{2}\right\} \\ \left\{-\frac{1}{2}, \frac{1}{2}, -\frac{1}{2}\right\} \end{matrix} \right) \right\}$$

$$+\frac{\sqrt{\tau'}}{\ln 2} G_{1,3}^{3,1}\left(\tau' \left| \begin{matrix} \left\{-\frac{1}{2}\right\} \\ \left\{-\frac{1}{2}, \frac{1}{2}, -\frac{1}{2}\right\} \end{matrix} \right.\right)$$

$$-\frac{\sqrt{\chi}}{\ln 2} \frac{d_{R,D_2}^{\nu}}{d_{R,D_1}^{\nu} + d_{R,D_2}^{\nu}} G_{1,3}^{3,1}\left(\chi \left| \begin{matrix} \left\{-\frac{1}{2}\right\} \\ \left\{-\frac{1}{2}, \frac{1}{2}, -\frac{1}{2}\right\} \end{matrix} \right.\right), \tag{3.22}$$

where $\tau' = \frac{d_{S,R}^{\nu} d_{R,D_2}^{\nu} \sigma^2}{\eta \rho P_s \beta_s}$. Note that $\bar{C}_{D_2}^{x_2}$ is obtained by exchanging d_{R,D_1} and d_{R,D_2} in $\bar{C}_{D_1}^{x_1}$.

3.3 End-to-End Ergodic Capacity

The end-to-end ergodic capacity of a relay network is determined by the weakest link between the source-to-relay link and relay-to-user link. The end-to-end ergodic capacity from the source to $D_k,\ k \in \{1,2\},$ is given by [20]

$$\bar{C}^{x_k} = \frac{1}{2}\min\{\bar{C}_R^{x_k}, \bar{C}_{D_k}^{x_k}\}. \tag{3.23}$$

Chapter 4

Simulation Results

Consider a downlink EH cooperative NOMA network with a source, a DF relay, and two users D_1 and D_2. Suppose that the power splitting ratio $\rho = 0.5.$ Assume that the energy conversion efficiency $\eta = 0.5,$ the noise variance $\sigma^2 = -86$ dBm, the path loss exponent $\nu = 3.5$, and the distance between the source and the relay $d_{S,R} = 10$ m, that between the relay and D_1 $d_{R,D_1} = 5$m, and that between the relay and D_2 $d_{R,D_2} = 10$ m. Suppose that the power allocation coefficients for the first and second time slot are given by $\alpha_w = \beta_w = 0.8$ and $\alpha_s = \beta_s = 0.2$.

Figure 4.1 shows the ergodic capacity versus the source transmit power for different values of the power allocation coefficient α_w. In Figure 4.1 (a), the power allocation coefficient $\alpha_w = 0.7$. In Figure 4.1 (b), the power allocation coefficient $\alpha_w = 0.8$. In Figure 4.1 (c), the power allocation coefficient $\alpha_w = 0.9$. In Figure 4.1 (d), the power allocation coefficient $\alpha_w = 0.95$. It is shown that both end-to-end capacities from the source to the user increases as P_S increases. It is also shown that the end-to-end capacity from the source to D_1 is always larger than that from the source to D_2. For the fairness between the users, large α_w is desired.

Figure 4.2 shows the ergodic capacity versus the power allocation coefficient α_w for different values of the source transmit power P_S. In Figure 4.2 (a), the source transmit power $P_S = 20$ dBm. In Figure 4.2 (b), the source transmit power $P_S = 10$ dBm. In Figure 4.2 (c), the source transmit power $P_S = 0$ dBm. It is shown that the end-to-end ergodic capacity from the source to D_1 decreases as α_w increases while that from the source to D_2 increases. It is also shown that the ergodic sum capacity decreases as α_w increases.

Figure 4.3 shows the ergodic capacity versus the power splitting ratio ρ for different values of the source transmit power P_S. P_S. In Figure 4.3 (a), the source transmit power $P_S = 20$ dBm. In Figure 4.3 (b), the source transmit power $P_S = 10$ dBm. In Figure 4.3 (c), the source transmit power $P_S = 0$ dBm. Note that both end-to-end capacities from the source to the users for $\rho = 0$ and $\rho = 1$ are given by 0. It is shown that the end-to-end from the source to the two users first increases and then decrease after their peaks as ρ increases. The reason is that the ergodic capacities from the source to relay decreases as ρ increases while that from the source to the users increases, and the end-to-end ergodic capacity is determined by the weakest link between the source-to-relay link and relay-to-user link.

Figure 4.4 shows the ergodic capacity versus the distance between the source to D_2 $d_{S,R}$ for different values of the path loss exponent v. In Figure 4.4 (a), the path loss exponent v =3.1. In Figure 4.4 (b), the path loss exponent v =3.5. In Figure 4.4 (c), the path loss exponent v =2.7. It is shown that the end-to-end ergodic capacity from the source to D_1 decreases as d_{R,D_2} increases while that from the source to D_2 increases.

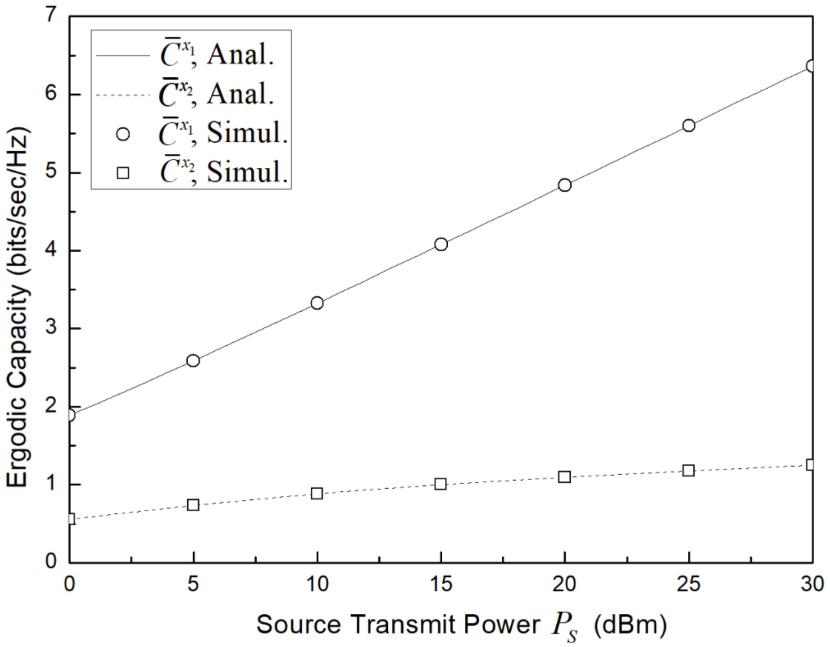

$\bar{C}^{x_1}$, Anal.
$\bar{C}^{x_2}$, Anal.
$\bar{C}^{x_1}$, Simul.
$\bar{C}^{x_2}$, Simul.
Ergodic Capacity (bits/sec/Hz)
Source Transmit Power P_S (dBm)
0
1
2
3
4
5
6
7
0
5
10
15
20
25
30

(a) $\alpha_w = 0.7$

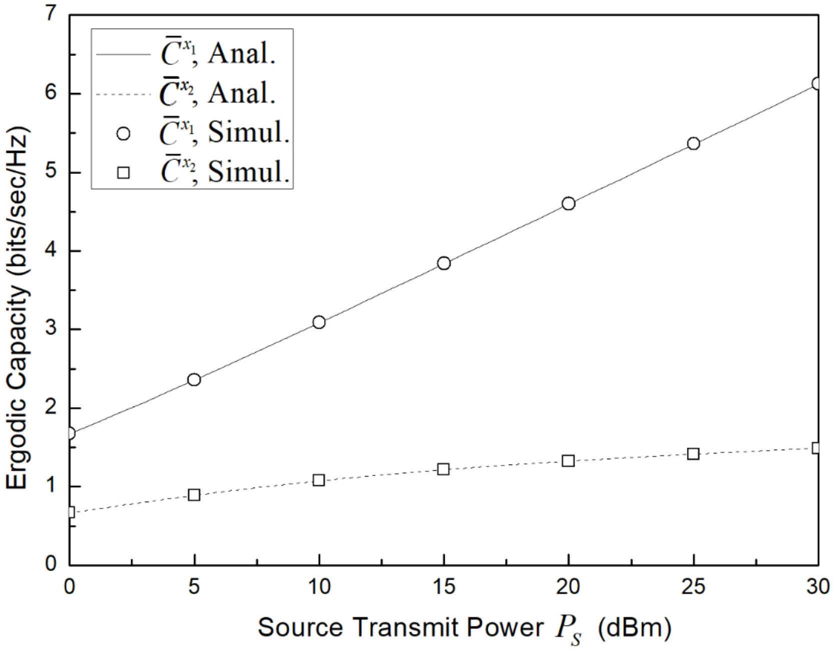

$\bar{C}^{x_1}$, Anal.
$\bar{C}^{x_2}$, Anal.
$\bar{C}^{x_1}$, Simul.
$\bar{C}^{x_2}$, Simul.
Ergodic Capacity (bits/sec/Hz)
Source Transmit Power P_S (dBm)
0
1
2
3
4
5
6
7
0
5
10
15
20
25
30

(b) $\alpha_w = 0.8$

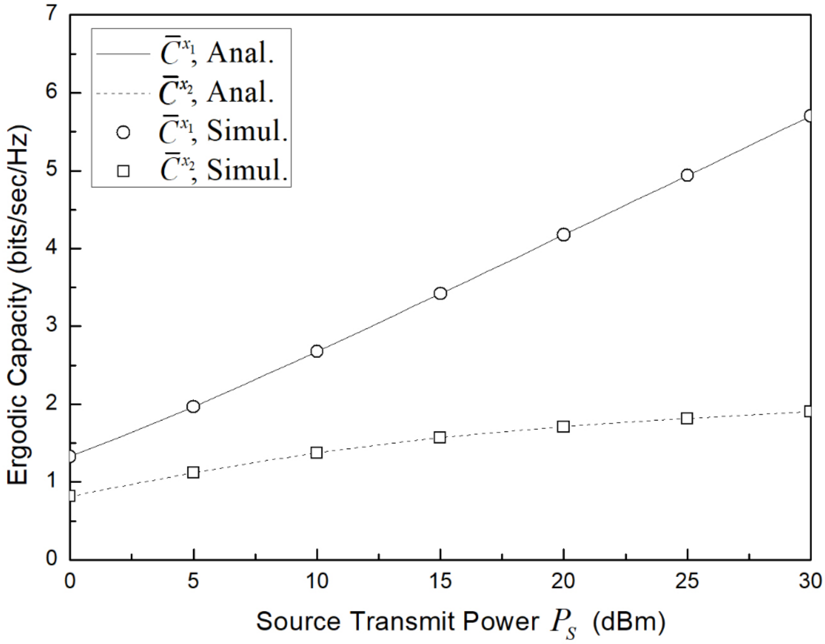

$\bar{C}^{x_1}$, Anal.
$\bar{C}^{x_2}$, Anal.
$\bar{C}^{x_1}$, Simul.
$\bar{C}^{x_2}$, Simul.
Ergodic Capacity (bits/sec/Hz)
Source Transmit Power P_S (dBm)
0
1
2
3
4
5
6
7
0
5
10
15
20
25
30

(c) $\alpha_w = 0.9$

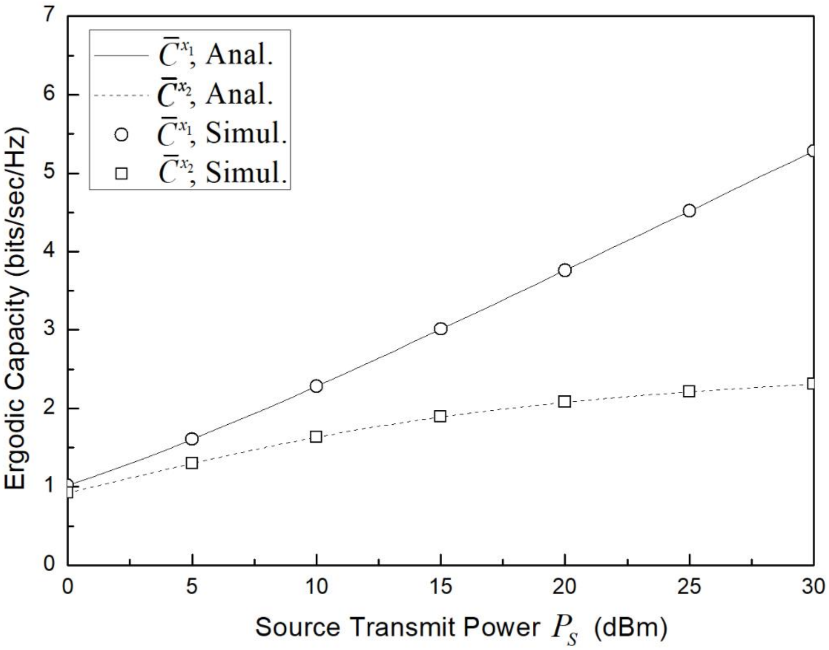

(d) $\alpha_w = 0.95$

Figure 4.1. Ergodic capacity versus the source transmit power P_S for different values of the power allocation coefficient α_w.

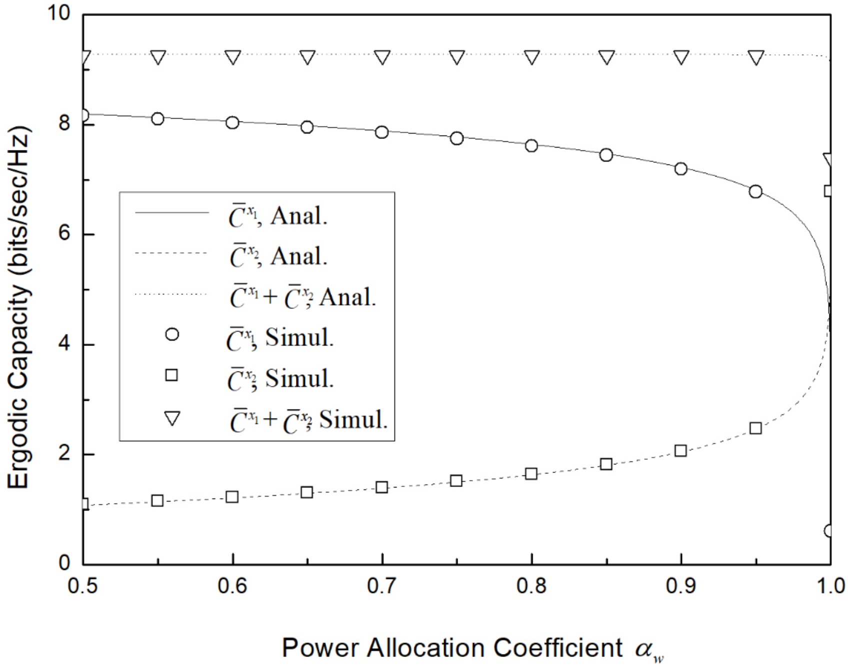

10
8
6
4
2
0
0.5
0.6
0.7
0.8
0.9
1.0
Ergodic Capacity (bits/sec/Hz)
Power Allocation Coefficient α_w
$\bar{C}^{x_1}$, Anal.
$\bar{C}^{x_2}$, Anal.
$\bar{C}^{x_1}+\bar{C}^{x_2}$, Anal.
$\bar{C}^{x_1}$, Simul.
$\bar{C}^{x_2}$, Simul.
$\bar{C}^{x_1}+\bar{C}^{x_2}$, Simul.

(a) $P_S = 20$ dBm

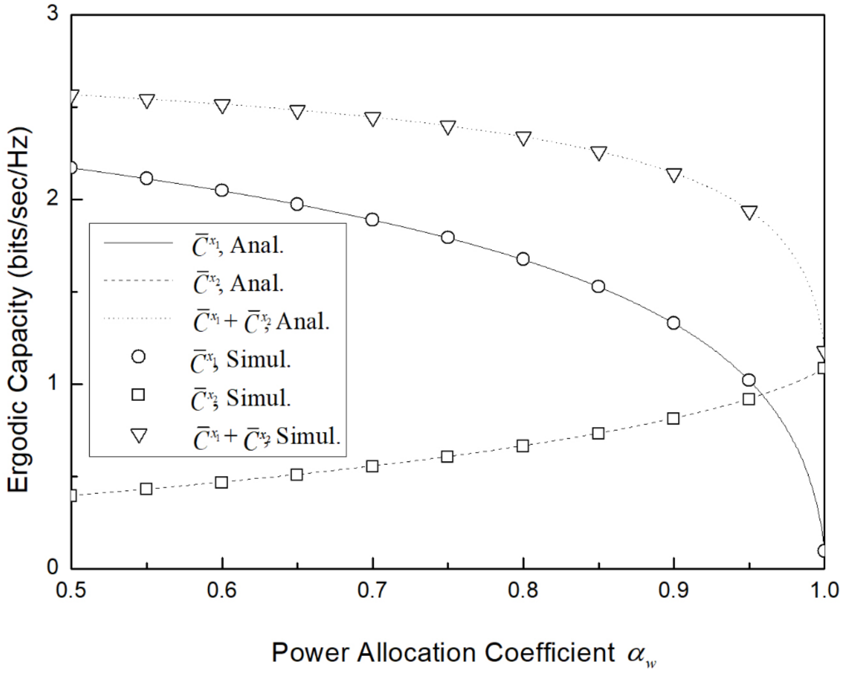

3
2
1
0
0.5
0.6
0.7
0.8
0.9
1.0
Ergodic Capacity (bits/sec/Hz)
Power Allocation Coefficient α_w
$\bar{C}^{x_1}$, Anal.
$\bar{C}^{x_2}$, Anal.
$\bar{C}^{x_1} + \bar{C}^{x_2}$, Anal.
$\bar{C}^{x_1}$, Simul.
$\bar{C}^{x_2}$, Simul.
$\bar{C}^{x_1} + \bar{C}^{x_2}$, Simul.

(b) $P_S = 10$ dBm

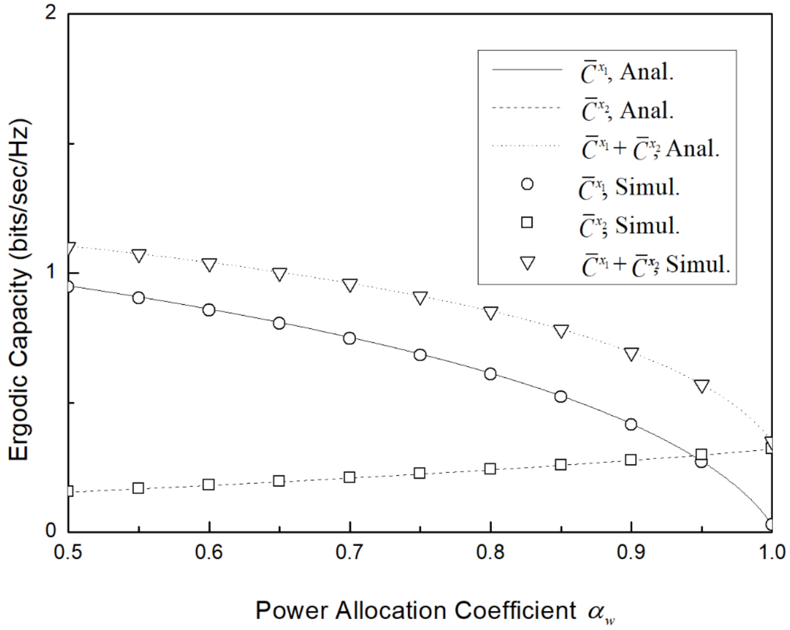

(c) $P_S = 0$ dBm

Figure 4.2. Ergodic capacity versus the power allocation coefficient α_w for different values of the source transmit power P_S.

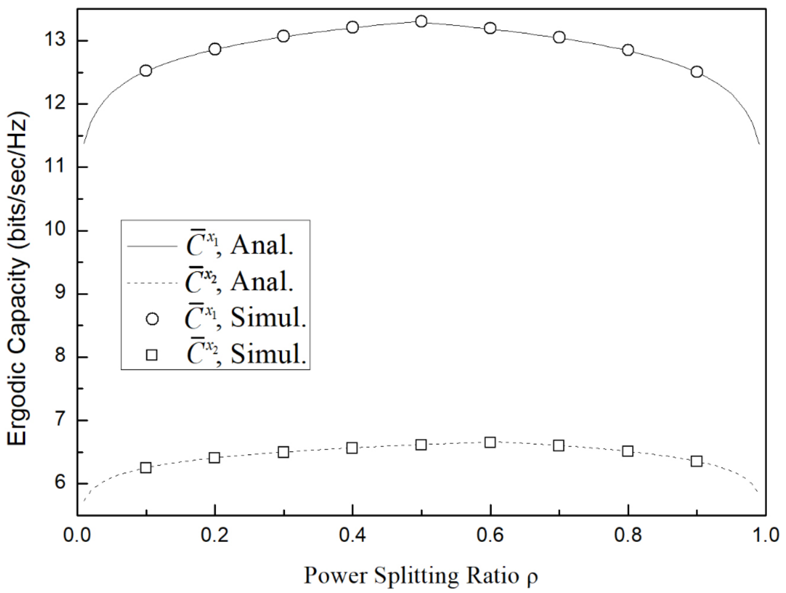

13
12
11
10
9
8
7
6
0.0
0.2
0.4
0.6
0.8
1.0
Ergodic Capacity (bits/sec/Hz)
Power Splitting Ratio ρ
$\bar{C}^{x_1}$, Anal.
$\bar{C}^{x_2}$, Anal.
$\bar{C}^{x_1}$, Simul.
$\bar{C}^{x_2}$, Simul.

(a) $P_S = 20$ dBm

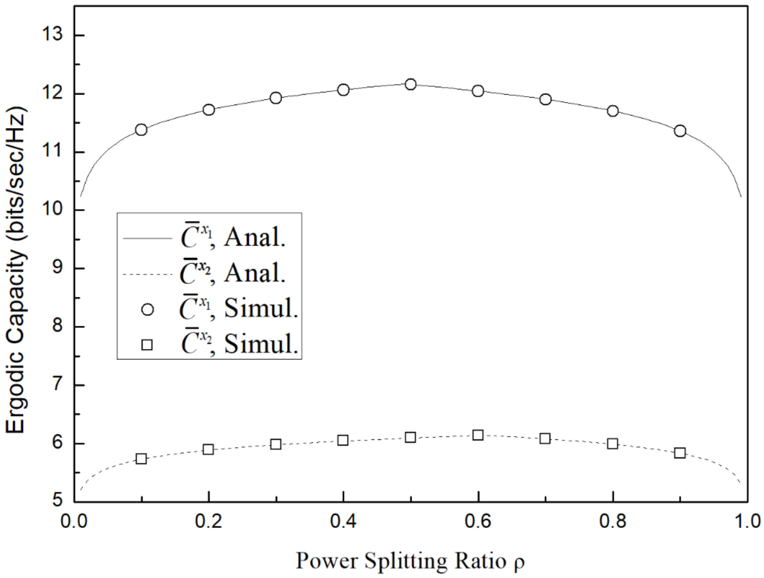

13
12
11
10
9
8
7
6
5
0.0
0.2
0.4
0.6
0.8
1.0
Ergodic Capacity (bits/sec/Hz)
Power Splitting Ratio ρ
$\overline{C}^{x_1}$, Anal.
$\overline{C}^{x_2}$, Anal.
$\overline{C}^{x_1}$, Simul.
$\overline{C}^{x_2}$, Simul.

(b) $P_S = 10$ dBm

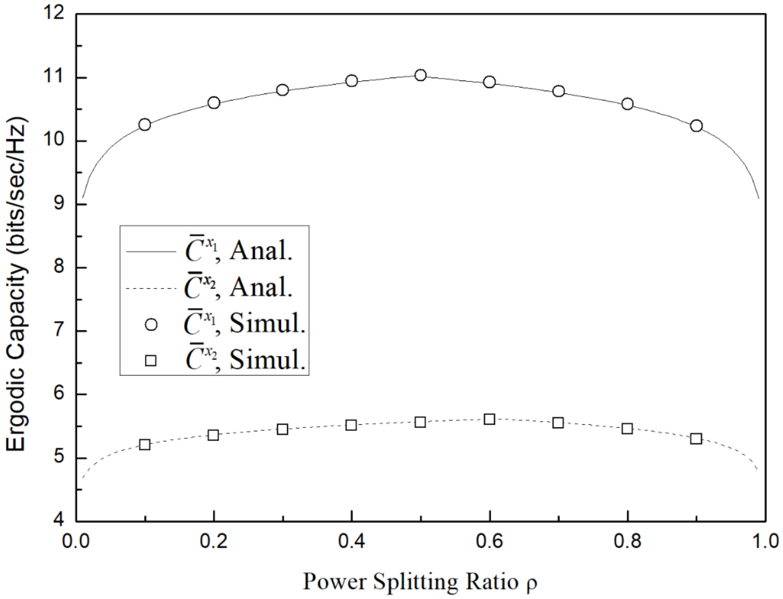

(c) $P_S = 0$ dBm

Figure 4.3. Ergodic capacity versus the power splitting ratio ρ for different values of the source transmit power P_S.

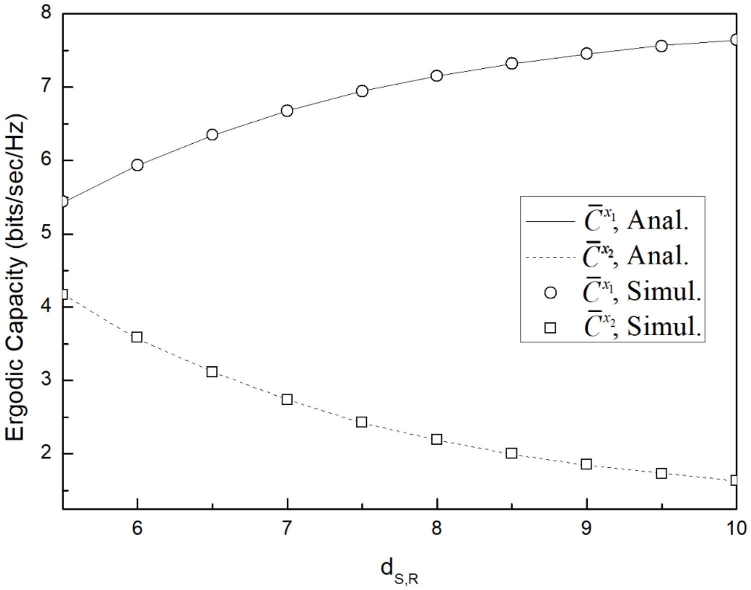

Ergodic Capacity (bits/sec/Hz)
$d_{S,R}$
$\bar{C}^{x_1}$, Anal.
$\bar{C}^{x_2}$, Anal.
$\bar{C}^{x_1}$, Simul.
$\bar{C}^{x_2}$, Simul.

(a) $\nu = 3.5$.

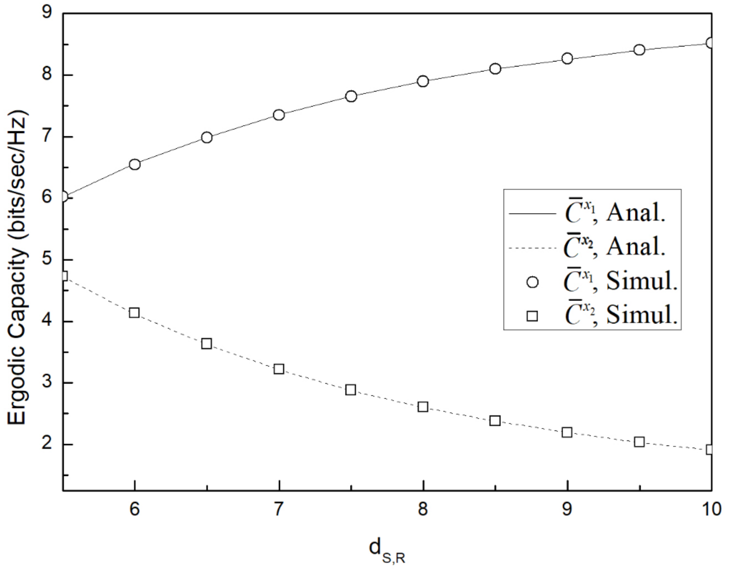

Ergodic Capacity (bits/sec/Hz)
9
8
7
6
5
4
3
2
6
7
8
9
10
$d_{S,R}$
$\bar{C}^{x_1}$, Anal.
$\bar{C}^{x_2}$, Anal.
$\bar{C}^{x_1}$, Simul.
$\bar{C}^{x_2}$, Simul.

(b) $\nu = 3.1$.

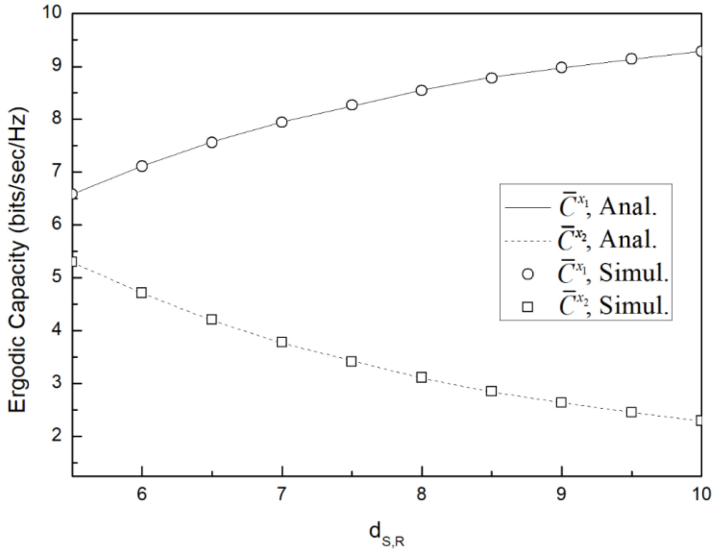

(c) $\nu = 2.7$.

Figure 4.4. Ergodic capacity versus the distance between the source to D_2 $d_{S,R}$ for different values of the path loss exponent ν.

Chapter 5

Conclusion

In this thesis, a downlink cooperative NOMA network with a decode-and-forward relay is investigated. A closed-form expression of the end-to-end capacities from the source to the two users are derived.

Channel order indicator is adopted to ensure that more power is allocated to the instantaneous weak user, according to the NOMA principle. To obtain the end-to-end capacities from the source to the users, the received SINRs at the relay and the users are derived. Then the CDFs of the SINRs are calculated, and finally the analytical expressions for the end-to-end ergodic capacities between the source and the users are derived. Simulation results show that the ergodic capacities of the users increase as the source transmit power increases. It is also shown that the end-to-end ergodic capacity from the source to the user closer to the relay decreases as the power allocation coefficient for the weak user increases while that from the source to the user farther to the relay increases.

Bibliography

[1] Z. Ding, Z. Yang, P. Fan, and H. V, Poor, ”On the performance of nonorthogonal multiple access in 5G systems with randomly deployed users,” *IEEE Signal Process. Lett.*, vol. 21, no. 12, pp. 1501-1505, Dec. 2014.

[2] Z. Ding, Y. Li, J. Choi, Q. Sun, M. Elkashlan, C. I, and H. V. Poor, “Application of non-orthogonal multiple access in LTE and 5G systems,” *IEEE Commun. Mag.*, vol. 55, no. 2, pp. 185-191, Feb. 2017.

[3] M. Salem, A. Adinoyi, H. Yanikomeroglu, and D. Falconer, “Opportunities and challenges in OFDMA-based cellular relay networks: a radio resource management perspective,” *IEEE Trans. Veh. Technol.,* vol. 59, no. 5, pp. 2496-2510, June 2010.

[4] I. Lee and D. Kim, “Coverage extension and power allocation in dual-hop space–time transmission with multiple antennas in each node,” *IEEE Trans. Veh. Technol.,* vol. 56 no. 6 pp. 659-672, July 2006.

[5] A. Bletsas, A. Khisti, D. P. Reed, and A. Lippman, “A simple cooperative diversity method based on network path selection,” *IEEE J. Sel. Areas Commun.*, vol. 24, no. 3, pp. 1606-1618, Mar. 2006.

[6] D. Cao, S. Zhou, C. Zhang, and Z. Niu, “Energy saving performance comparison of coordinated multi-point transmission and wireless relaying,” *IEEE Trans. Wireless Commun*., vol. 13, no. 3, pp. 1499-1513, Mar. 2014.

[7] J. Kim and I. Lee, “Capacity analysis of cooperative relaying systems using non-orthogonal multiple access,” *IEEE Commun. Lett.*, vol. 19, no. 11, pp. 1949-1952, Nov. 2015.

[8] L. Lv, J. Chen, Q. Ni, and Z. Ding, “Design of cooperative non-orthogonal multicast cognitive multiple access for 5G systems: user scheduling and performance analysis,” *IEEE Trans. Commun*., vol. 65, no. 6, pp. 2641-2656, June 2017.

[9] Y. Li, M. Jiang. Q. Zhang, Q. Li, and J. Qin, “Cooperative Non-orthogonal multiple access in multiple-input-multiple-output channels,” *IEEE Trans.*

Wireless Commun., vol. 17, no. 3, pp. 2068-2079, Mar. 2018.

[10] X. Chen, X. Wang, and X. Chen, “Energy-efficient optimization for wireless information and power transfer in large-scale MIMO systems employing energy beamforming,” *IEEE Wireless Commun. Lett*, vol. 2, no. 6, pp. 667-670, Dec. 2013.

[11] Q. Li, Q. Zhang, and J. Qin, “Beamforming in non-regenerative two-way multi-antenna relay networks for simultaneous wireless information and power transfer,” *IEEE Trans. Wireless Commun.*, vol. 13, no. 10, pp. 5509-5520, Oct. 2014.

[12] Y. Xu, C. Shen, Z. Ding, X. Sun, S. Yan, G. Zhu, and Z. Zhong, “Joint beamforming and power-splitting control in downlink cooperative SWIPT NOMA systems,” *IEEE Trans. Signal Process.*,vol. 65, no. 18, pp. 4874-4886, Sep. 2017.

[13] Y. Liu, Z. Ding, M. Elkashlan, and H. V. Poor, “Cooperative non-orthogonal multiple access with simultaneous wireless information and power transfer,” *IEEE J. Sel. Areas Commun*., vol. 34, no. 4, pp. 436-453, Apr. 2016.

[14] Z. Yang, Z. Ding, P. Fan, and N. Al-Dhahir, “The impact of power allocation on cooperative non-orthogonal multiple access networks with

SWIPT," *IEEE Trans. Wireless Commun.*, vol. 16, no. 7, pp. 4332-4343, July 2017.

[15] R. W. Heath, Jr., N. Gibzakez-Prelcic, S. Rangan, W. Roh, and A. M. Sayeed, "An overview of signal processing techniques for millimeter wave MIMO systems," *IEEE J. Sel. Areas Commun*., vol. 10, no. 3, pp. 436-453, Apr. 2016.

[16] Q. Wang, J. Ge, Q. Li, and Q. Bu, "Performance analysis of NOMA for multiple-antenna relaying networks with energy harvesting over Nakagami-*m* fading channels," in *Proc. IEEE Int. Conf. Commun. in China (ICCC),* Chengdu, China, Oct. 2017, pp. 1-5.

[17] Y. Zhang and J. Ge, "Performance analysis for non-orthogonal multiple access in energy harvesting relaying networks," *IET Commun*., vol. 11, no. 11, pp. 1768-1774, Nov. 2017.

[18] Y. Zhang, J. Ge, and E. Serpedin, "Performance analysis of a 5G energy-constrained downlink relaying network with non-orthogonal multiple access," *IEEE Trans. Wireless Commun*., vol. 16, no. 12, pp. 8333-8346, Dec. 2017.

[19] I. S. Gradshteyn and I. M. Ryzhik, "*Table of Integrals, Series, and Products*," 6/e, San Diego, CA: Academic, 2000

[20] V. S. Adamchik and O. I. Marichev, ″The algorithm for calculating integrals of hypergeometric type functions and its realization in REDUCE system,” in *Proc. ACM Int. Symp. Symbolic Algebraic Comput.*, Tokyo, Japan, Aug. 1990, pp. 212-224.

[21] A. A. Nasir, X. Zhou, S. Durrani, and R. A. Kennedy, “Relaying protocols for wireless energy harvesting and information processing,” *IEEE Trans. Wireless Commun.*, vol. 12, no. 7, pp. 3622-3636, July 2013.

Korean Abstract

본 논문에서는 에너지 하베스팅과 복호 후 전달 방식을 사용하는 중계기가 있는 비직교 다중접속 시스템에 대해 연구한다. 송신기와 중계기 사이 및 중계기와 수신기 사이의 신호대간섭잡음비의 누적분포함수을 유도하여 시스템의 단대단 에르고딕 전송 용량을 분석한다. 모의 실험을 통해 시스템의 단대단 에르고딕 전송 용량의 분석 결과가 실험 결과와 일치함을 확인한다.

주요어: 비직교 다중접속, 협력통신, 에너지 하베스팅, 복호 후 전달. 파워 분할.

학번: 2017-23534

Acknowledgements

석사 학위를 받기까지 지난 2년간 도움을 주신 분들께 이 지면을 빌려 감사의 말씀을 드리고자 합니다.

먼저 본 논문이 있기까지 저를 지도해주시고 이끌어 주신 이재홍 교수님께 감사드립니다. 또한 바쁘신 와중에도 논문 심사를 맡아 지도해 주신 이정우 교수님, 최성현 교수님께 감사드립니다. 그리고 지금까지 배움의 길을 열어 주신 서울대학교 전기정보공학부 여러 교수님들께 감사드립니다.

석사과정 동안 많은 것을 알려주시고 제 부족한 점들을 채워 주신 통신 및 부호이론 연구실 선배님들께 진심으로 감사드립니다. 가장 힘들 때 위로를 해 주시고 연구를 해 나갈 수 있도록 길을

알려주신 주현이형, 경래형, 용윤이형, 승근이형에게 감사드립니다.

항상 저를 믿고 지켜봐 주시는 부모님께 감사드립니다. 제가 잘 하든 못하든 언제나 저를 응원해 주시고 제가 힘들 때는 같이 고민해 주시는 부모님 덕분에 여기까지 올 수 있었습니다. 늘 감사하고 사랑합니다. 제 인생의 가장 오랜 벗인 동생에게도 감사의 마음을 전합니다.

그동안 제게 많은 관심과 격려, 그리고 힘을 주신 분들께 다시 한 번 큰 감사를 드리며, 저를 신경 써주시는 모든 분들에게 감사한 마음을 전합니다.